PAPER

Check for updates

Synchronous oxidation and sequestration for As(III) from aqueous solution by modified CuFe₂O₄ coupled with peroxymonosulfate: a fast and stable heterogeneous process†

Fu Liu, Jian-Feng Wu and Guang-Chao Zhao [iD] *

Bifunctional heterogeneous catalytic processes for highly efficient removal of arsenic (As(III)) are receiving increased attention. However, the agglomerated nature and stability of nanoparticles are major concerns. Herein, we report a new process regarding the anchoring of CuFe₂O₄ nanoparticles on a substrate material, a kind of Fe–Ni foam, to form porous CuFe₂O₄ foam (CuFe₂O₄-foam) by *in situ* synthesis. The prepared material was then applied to activate peroxymonosulfate (PMS) for fast and efficient removal of As(III) from water. The results of removal experiments show that the complete removal of arsenic (<10 μg L^{-1}) from 1 mg L^{-1} As(III) aqueous solution can be achieved within shorter time (<10 min) using this adsorbent coupled with PMS. The maximum adsorption capability of As(III) and As(v) on the prepared adsorbent is observed to be about 105.78 mg g^{-1} and 120.32 mg g^{-1}, respectively. CuFe₂O₄-foam/PMS couple could work effectively in a wide pH range (3.0–9.0) and temperature range (10–60 °C), which is more beneficial to its application in actual water treatment engineering. The exhausted adsorbents can be refreshed for cyclic runs (at least 7 cycles) with insignificant capacity loss using alkaline solution as a regeneration strategy, suggesting this process has good stability. Investigation of the mechanism reveals that the route to the removal of As(III) is synchronous oxidation and sequestration in the arsenic removal process. The large As(III) removal capability and stability of CuFe₂O₄-foam/PMS show its potential as a promising candidate in real As(III)-contaminated groundwater treatment.

1. Introduction

Among various heavy metals found in natural groundwater, naturally occurring arsenic is a major public issue threatening millions of people worldwide. Given the potential hyper-toxicity, bio-accumulation, and environmental persistence of arsenic even at trace levels, various environmental protection agencies and national bodies have regulated the maximum limit of arsenic in water for safe drinking as 10 μg L^{-1}.[1,2] Water contamination by arsenic is a serious and ubiquitous global problem, especially in some developing regions, such as Bangladesh and China.[3–5] Due to the huge threat of arsenic on human health, reliable and economical methods are urgently needed for its efficient removal from water.

Numerous techniques, such as precipitation, ion exchange, coagulation, membrane separation and adsorption has been developed for arsenic removal from contaminated water,[6,7] among which adsorption is an promising method due to its simplicity of operation and low cost.[8,9] However, the adsorption is effective only for As(v) but not valid for As(III).[10] Noted that the dominant species of arsenic in aqueous environment is As(III) and is much higher mobility and toxicity than inorganic As(v).[11,12] Thus, preoxidation of As(III) to As(v) is an usually regarded as a effective strategy to enhance the removal of As(III).[13–15] Nowadays, in order to integrate oxidation and adsorption processes for the removal of As(III), considerable efforts have been devoted to developing new materials and technology.[15–18] Among them, heterogeneous catalytic process, which based on advanced oxidation processes (AOPs), attracted increasing interest due to some promising results in the fast and efficient removal of both arsenic and organic contaminants in water.[19–22]

Recently, various nanosized metal oxide adsorbents, such as Al(III),[19] Fe(III),[20,21] Cu(II)(hydr)oxides,[22] have been proposed for the above purpose, among which iron oxide nanoparticles is the most extensively concerned material because of their good performance, readily availability and environmental friendliness. Compared to other iron-based materials, spinel-type particle (CuFe₂O₄, CoFe₂O₄, *etc.*) is very promising taken into account its excellent properties, such as the high catalytic activity and mechanical stability.[23,24] However, nanoparticles are

School of Ecology and Environment, Anhui Normal University, Wuhu 241000, P. R. China. E-mail: gczhao@mail.ahnu.edu.cn

† Electronic supplementary information (ESI) available. See DOI: 10.1039/d0ra09324f

prone to agglomeration, which dramatically decreases their specific surface area and accessible reactive sites.[25] Moreover, the separation of adsorbent powder after completing the removal from treated water is still a challenge or inconvenient, although nanoparticles can be centrifugally separated, filtrated or external magnetic field.[26] The complicated post-treatment steps are easy to cause secondary disposal and contamination for water. Various strategies, such as fabricating porous catalysts and anchoring nanoparticles on substrate materials, have been investigated for preventing the agglomeration of its.[25,27–30] For example, Sun *et al.* prepared monodispersed $CuFe_2O_4$ nanoparticles anchored on natural kaolinite as highly efficient peroxymonosulfate catalyst.[25] It is therefore of great needs to develop stable and recyclable catalyst combined with large adsorption capacity to improve the overall efficiency of removal arsenic by minimizing the required dosage of adsorbents. Taking into account of the stability of metal substrate, anchoring $CuFe_2O_4$ nanoparticles on the surface of on Fe–Ni framework is expected to be an economical and efficient heterogeneous catalyst for coupling oxidation and adsorption arsenic.

This work reports the synthesis and characterization of $CuFe_2O_4$ nanoparticles anchored on the surface of Fe–Ni framework followed by the evaluation of the aforementioned catalyst coupled with peroxymonosulfate (PMS) for removal of As(III), particularly in complex aqueous environment. Moreover, the active oxygen species responsible for the oxidation of As(III) were investigated through a series of quenching experiments, and the potential reaction mechanisms for the promising removal property of this couple were proposed. Finally, the removal efficiency of As(III) at low concentration ($\sim$1 mg L^{-1}) in practical water samples were estimated under seven regenerative or consecutive tests. The results of experiment suggested that the joint method may provide a option to fast and efficiently remove the low concentration arsenic contaminant without adjusting the substances in water.

2. Experimental section

2.1. Reagents

As(III) and As(V) stock solutions (1.0 g L^{-1}), peroxymonosulfate ($KHSO_5\cdot0.5KHSO_4\cdot0.5K_2SO_4$), 5,5-dimethyl-1-pyrroline N-oxide (DMPO) were purchased from J&K Chemical Company. *tert*-Butyl alcohol ($C_4H_{10}O$, TBA), ethanol (C_2H_6O, EtOH), humic acid (HA), copper nitrate trihydrate ($Cu(NO_3)_2\cdot3H_2O$), Iron nitrate nonahydrate ($Fe(NO_3)_3\cdot9H_2O$) and urea ($CO(NH_2)_2$) were purchased from Macklin Biochemical Co., Ltd (Shanghai, China). Fe–Ni foam framework was produced from Anhui PuYu Technology Co., Ltd. All of above mentioned are of analytical reagent grade and used asreceived. Stock solutions were always prepared in ultrapure water produced by a Milli-Q system.

2.2. Characterization

The crystal phases of the particles were identified by X-ray diffraction (XRD, Bruker D8 Advance, Germany) using a CuKα X-ray radiation source, and the operation voltage and current

were 40 kV and 40 mA, respectively. The surface morphology and elemental mappings were examined by field emission scanning electron microscope mounted with an energy dispersive X-ray spectroscopy (FESEM, Hitachi SU-8010, 5 kV, Japan). X-ray photoelectron spectroscopy determined the surface chemistry properties of the adsorbent (XPS, Thermo Escalab 250XI, American). BET surface area and average pore size of the oxides were determined on a JW-BK 112 analyzer. The point of zero charge (PZC), at which a solid submerged in an electrolyte exhibits zero net electrical charge on the surface, was measured by pH drift method.[31]

2.3. Preparation of adsorbent

$CuFe_2O_4$-foam was prepared by *in situ* synthesis refereeing previous reports, and described in details as following.[32] Fe–Ni foam framework (approximately 20 mm × 20 mm × 2 mm, one piece) was firstly immersed into 4.0 M HCl solution for 3 min to remove the surface oxide layer, further washed by ethanol and ultrapure water and then dried in 80 °C. The $CuFe_2O_4$ nanoparticles *in situ* anchored on Fe–Ni foam framework were synthesized by a hydrothermal method. In brief, the molar ratio 1 : 2 : 5 of copper nitrate, iron nitrate and urea were dissolved into 100 mL of ultrapure water under magnetic stirring for 2 h to form a mixed solution. After that the obtained homogeneous solution was transferred into a 200 mL Teflon-lined stainless steel autoclave, the pretreated Fe–Ni foam framework was immersed to mixture, and then the autoclave was maintained in an oven at 150 °C for 6 h to generate the product denoted as $CuFe_2O_4$-foam. Finally, the resulted black $CuFe_2O_4$-foam was washed with ultrapure water until the pH reached neutral and dried at 80 °C for 2 h.

2.4. Procedures of batch, As concentration determination, and regenerative tests

A common stock solution of each reactant was prepared and aliquots of the stock solutions were combined to achieve the initial experimental conditions. Batch adsorption experiments were carried out in 100 mL Erlenmeyer flasks. Specific amounts of $CuFe_2O_4$-foam and PMS solution were initially dispersed into 80 mL solution with 0.5 mM Na_2SO_4 as the background electrolyte. After mixing for 1 min, a certain dosage of As(III) stock solution was added to start the reaction. Unless otherwise specified, the temperature of all batch experiments was set at 25 ± 2 °C in a constant-temperature water bath oscillator with the stirring rate 150 rpm under exposure to air, and the initial pH values (pH$_0$) of aqueous solution were adjusted to 7.0 ± 0.5 with HNO$_3$ or NaOH solution, and no attempt was made to maintain a constant pH during the experiments.

For all the arsenic removal experiments, samples were withdrawn through 0.45 μm membrane filter at predetermined time intervals. To accurately analyze the concentration of arsenic, excess sodium nitrite was immediately introduced into the filtrate to exhaust the residual PMS. The concentration of As(III) was determined by an atomic fluorescence spectrophotometer (AFS-9700, Shimadzu, Japan). The As(V) concentration in solution were estimated by using the modified molybdate-

based method described in references, and the details are present in Text S1.†[33] Each experiment was performed in triplicate, and the average results were reported.

After material regeneration, the adsorption capacity for arsenic was studied to evaluate the reusability of prepared $CuFe_2O_4$-foam. A piece of $CuFe_2O_4$-foam was firstly in contact with 80 mL 1 mg L^{-1} arsenic solution at pH_0 7.0, then the adsorbent was removed and washed with ultrapure water to remove the excessive arsenic in the surface. For regeneration test, the removed $CuFe_2O_4$-foam was contacted with 5% NaOH for 6 h to desorb the adsorbed arsenic, then washed and dried at 80 °C for 2 h. The regenerated adsorbent was used for the next adsorption–desorption cycle experiment.

3. Results and discussion

3.1. Analysis and material characterization

The Fe–Ni framework precursors are gray lumps of around 20 mm in side length and 2 mm in thickness and the prepared $CuFe_2O_4$-foam remain the shape and size of their precursors but presents as a black color (Fig. S1†). As $CuFe_2O_4$ anchored on Fe–Ni framework, an obvious increase in BET surface area is observed from 2.769 $m^2 g^{-1}$ to 5.831 $m^2 g^{-1}$, which is believed to arise from the high BET surface area of the $CuFe_2O_4$. Furthermore, the average pore size rises to 13.98 nm of $CuFe_2O_4$-foam, as compared to Fe–Ni framework with 7.81 nm. Such change in the pore size distribution is mainly attributed to the partial formation of the new pore structure by the loaded $CuFe_2O_4$ nanoparticles. As shown in Fig. 1, the morphology and microstructure with or without $CuFe_2O_4$ loading were examined by

FESEM. The Fe–Ni framework is smooth and full of three-dimensional interconnected holes, which is believed to be beneficial for the enhancement of arsenic removal capacity (Fig. 2a and b). After $CuFe_2O_4$ nanoparticles randomly anchored on framework, its thickness was increased remarkably. Abundant pits formation and higher roughness was observed from Fig. 2c and d, which probably dramatically improve the removal capacity of adsorbent.[34,35] Moreover, the crystalline phases of bare $CuFe_2O_4$ was obtained by XRD and the results are presented in Fig. S2.† The different peaks of $CuFe_2O_4$ located at 30.17° (220), 35.54° (311), 43.20° (400), 53.59° (422), 57.13° (511) and 62.74° (440) matched well with the cuprospinel phase ($CuFe_2O_4$, JCPDS no. 77-0010), revealing its good crystalline.

Furthermore, XPS measurements were also performed to determine the chemical state of Cu, Fe, and O on the surface of prepared $CuFe_2O_4$-foam to better understand the surface properties of the materials. Of note, peak assignment in XPS spectra was based on literature reported binding energies of Cu/Fe materials and the spectra of reference materials acquired under the same conditions as the samples.[35,36] As shown in the survey spectra (Fig. 2a), elements of Cu, Fe, O, and C are detected, whereas the presence of C element was attributed to adventitious contaminants.[25] Cu 2p spectra is depicted in Fig. 2b, similar to previous studies,[26,32] the peaks appearing at the binding energies of 932.1 eV and 952.2 eV are assigned to the Cu $2p_{3/2}$ and Cu $2p_{1/2}$ characteristic peaks of Cu(II) on octahedral sites, respectively. However, it is incomprehensible that a weak peak appearing at binding energies of 933.5 eV, it maybe infer the new peak could be attributed to Cu(I) due to the materials prepared under anoxia conditions. In the Fe 2p
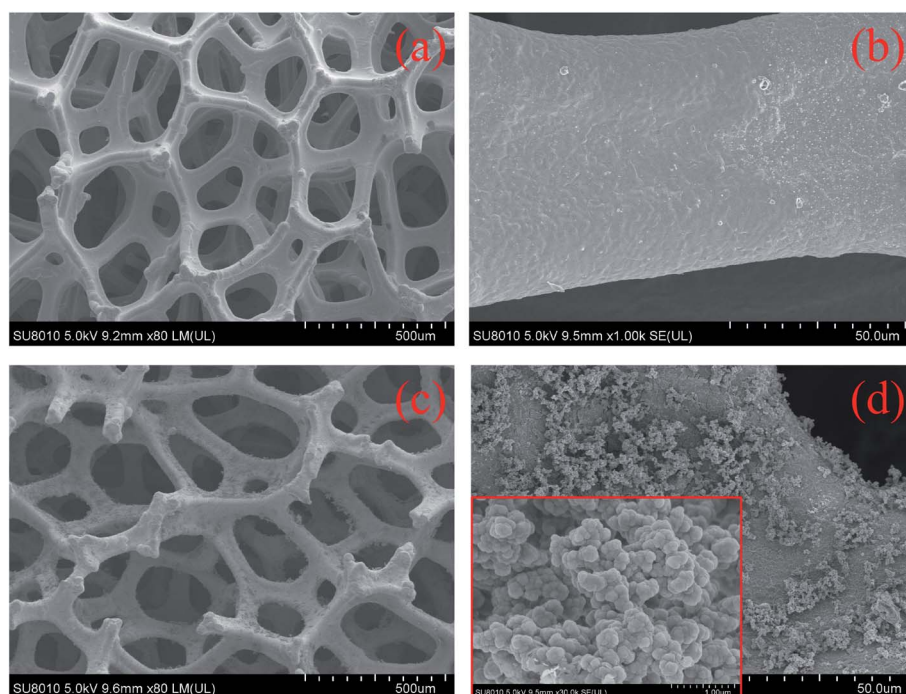

Fig. 1 SEM images of (a and b) Fe–Ni framework and (c and d) $CuFe_2O_4$-foam. The inset in (d) shows the high-magnification SEM image of loaded $CuFe_2O_4$.

© 2021 The Author(s). Published by the Royal Society of Chemistry
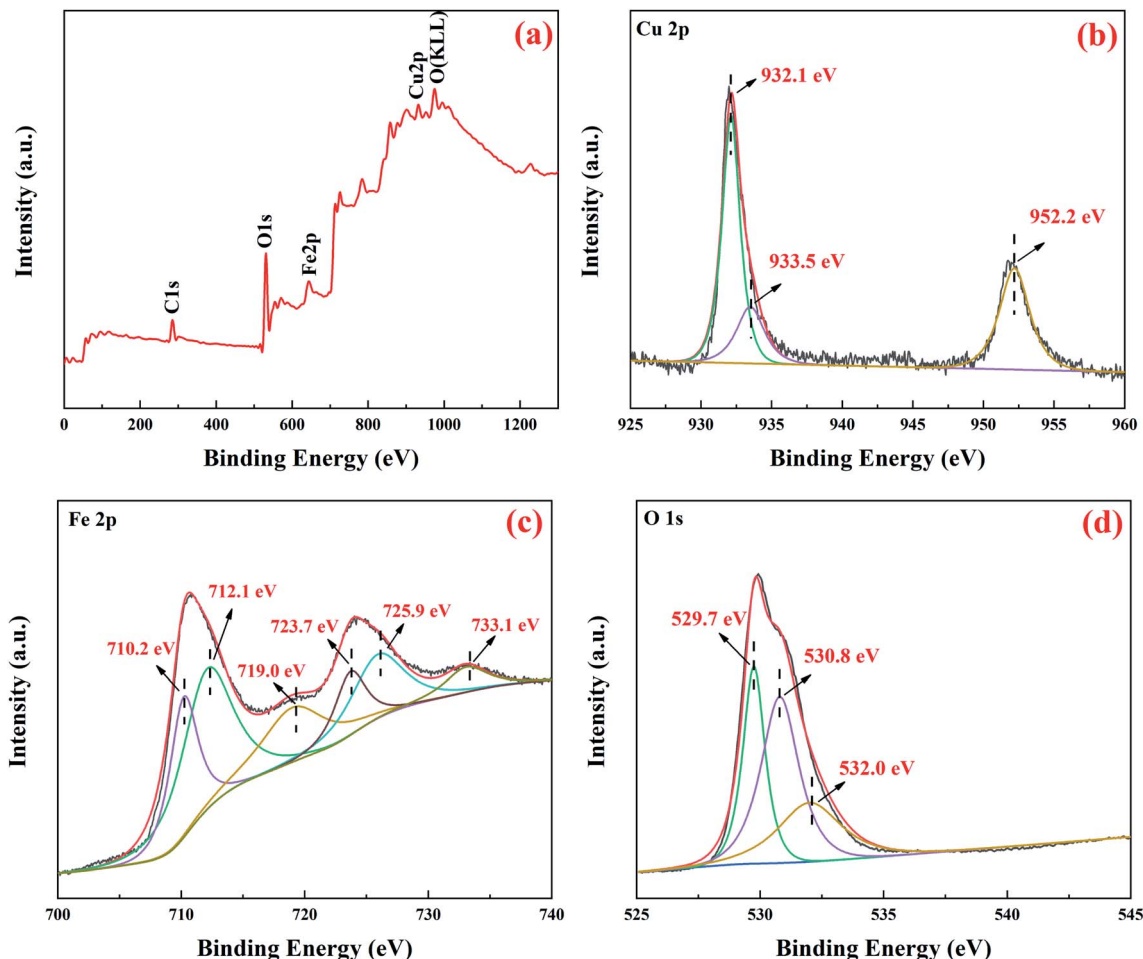
Paper

Fig. 2 XPS spectra of (a) survey, (b) Cu 2p, (c) Fe 2p, (d) O 1s for virgin $CuFe_2O_4$-foam.

spectra, the pristine peaks centered at 710.6 eV and 724.2 eV with a typical satellite peak at 719.0 eV, were consistent with the Fe $2p_{3/2}$ and Fe $2p_{1/2}$ of the Fe(III) state in the spin–orbit of $CuFe_2O_4$.[26,27,37] The peaks located at 710.2 eV and 723.7 eV are attributed to the Fe(III) in octahedral sites, while at binding energy of 712.1 eV and 725.9 eV could be ascribed to the Fe(III) in tetrahedral sites. XPS spectra of O 1s is presented in Fig. 2d, the main peaks centered at 529.7 eV, 530.8 eV and 532.0 eV, were attributed to lattice oxygen, surface hydroxyl groups and phys-isorption and/or chemisorbed water at/near the materials surface, respectively, similar to previous reports.[22,25,26]

3.2. As(III) removal performance by $CuFe_2O_4$-foam/PMS

3.2.1. Reactive activity of as-prepared adsorbents. After statistics of over 50 pieces prepared adsorbent, the average weight of one piece $CuFe_2O_4$-foam is ~539.3 mg, and the cor-responding mass of loaded $CuFe_2O_4$ is ~25.6 mg. The removal kinetic of As(III) by the $CuFe_2O_4$-foam composite coupled with PMS is displayed in Fig. 3. The arsenic species in solution were monitored, and all the residual arsenic is in the form of As(III). To demonstrate the crucial role of the addition of PMS, a comparative study was conducted to specify the role of each

related process involved in the arsenic removal. The kinetic data of As(III) removal are fitted by the pseudo-second order model (eqn (1)), and the detailed data were collected in Table S2.†

$$q_t = q_e \left(1 - \frac{1}{1 + q_e k_2 t} \right) \tag{1}$$

where q_t and q_e (mg g^{-1}) represent the adsorption capacity at time t (min) and at equilibrium, respectively. k_2 (g mg^{-1} min^{-1}) is the adsorption rate constants of pseudo-second-order, respectively.

Fig. 3a clearly present the promotion effect of PMS on As(III) removal, the adsorption was performed without PMS in first 20 min, and then added 100 μM PMS. Interestingly, the rapid As(III) removal was observed within 2 min compared with that in absence of PMS. More intuitive comparison was depicted in Fig. 3b, the k_2 value of $CuFe_2O_4$-foam/PMS couple (0.0168 g mg^{-1} min^{-1}) is obviously higher than that of $CuFe_2O_4$-foam alone (0.0032 g mg^{-1} min^{-1}) and $CuFe_2O_4$/PMS couple (0.0148 g mg^{-1} min^{-1}), with the residual As(III) concentration dropping dramatically from 10 mg L^{-1} to <10 μg L^{-1}. The fast adsorption equilibrium was obtained in 180 min with the addition of 100 μM PMS, while using $CuFe_2O_4$-foam alone required more than 360 min under otherwise identical conditions, which indicated
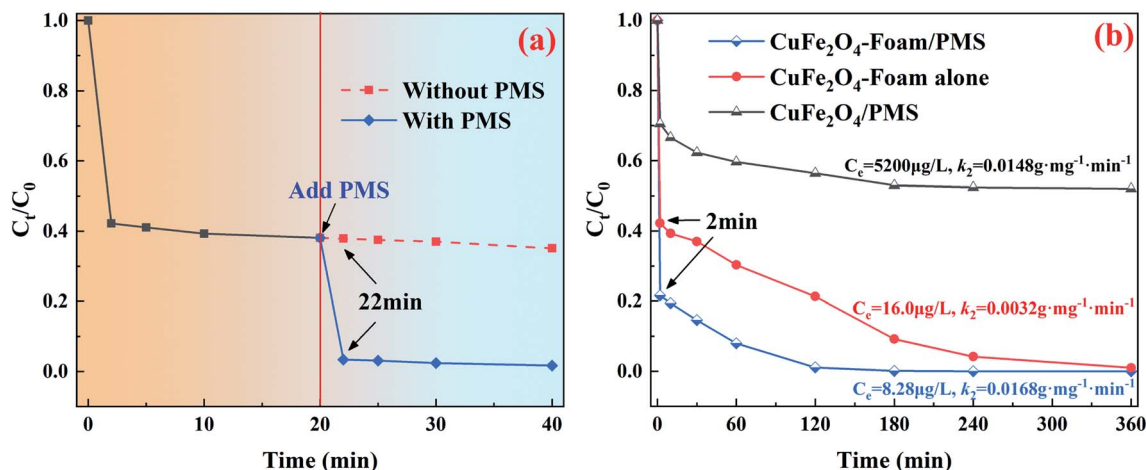
Fig. 3 As(III) or As(V) removal from aqueous solution, (a) the effect of PMS (100 μM) for As(III), (b) different adsorbent with or without PMS system for As(III). Conditions: 10 mg L^{-1} As(III), one piece adsorbent, 100 μM PMS, pH 7.0, 25 °C, 20 mg CuFe$_2$O$_4$ for (b).

the transformation of As(III) to As(V) is favorable for its sequestration by the embedded CuFe$_2$O$_4$-foam. Such enhancement in As(III) removal by CuFe$_2$O$_4$-foam/PMS couple possibly resulted from the oxidation of As(III) by its catalysis for PMS. Simultaneously, as shown in Fig. 3b, the abrupt As(III) removal occurred in 2 min, then the removal rate decreased slowly, also suggesting that there may be other elimination mechanisms besides adsorption. Compared with CuFe$_2$O$_4$/PMS couple, it can be inferred that the removal of As(III) by this system may be carried out *via* two pathways: one is the direct adsorption of As(III) and then situ oxidation because of the presence of oxidant, and the other is the oxidation of As(III) into As(V) in solution followed by As(V) adsorbed. The possible removal mechanism for As(III) by CuFe$_2$O$_4$-foam/PMS couple will be further discussed in the next section.

3.2.2. Removal isotherm. The removal isotherms of As(III) and As(V) by CuFe$_2$O$_4$-foam/PMS couple were both fitted by Langmuir and Freundlich adsorption models, as expressed in eqn (2) and (3), respectively, and the obtained adsorption parameters are listed in Table 1.

$$q_e = \frac{q_{max} K_L C_e}{1 + K_L C_e} \quad (2)$$

$$q_e = K_F C_e^{1/n} \quad (3)$$

where q_e is the As(III) capacity at equilibrium (mg g^{-1}) and q_{max} is the maximum adsorption capacity (mg g^{-1}), and C_e is the equilibrium concentration of arsenic (μg L^{-1}). K_L is the binding

constant (L mg^{-1}) of Langmuir model. K_F and n are adsorption constants and the heterogeneity factor of Freundlich model, respectively.

As depicted in Fig. 4, the CuFe$_2$O$_4$-foam/PMS couple shows the expected maximum adsorption capacity for both As(III) and As(V), which are 105.78 mg g^{-1} and 120.32 mg g^{-1}, respectively. The maximum adsorption capacity is much higher than that of bare CuFe$_2$O$_4$/PMS couple, which are 63.9 mg g^{-1} and 45.5 mg g^{-1} for As(III) and As(V), respectively.[22] The higher correlation coefficients of Langmuir model suggests that a monolayer coverage adsorption on heterogeneous adsorption sites in this process.[26] Of note, CuFe$_2$O$_4$-foam/PMS couple possesses a slight higher q_{max} but a much lower value of K_L for As(V) than that of As(III) (0.875 *vs.* 1.575 L mg^{-1}). Some reports had demonstrated the close relation of K_L with the affinity to a given pollutant.[38] The greatly enhanced K_L value apparently implied a much stronger affinity of CuFe$_2$O$_4$-foam/PMS couple with As(III) than with As(V), similar to previous studies.[15] Thereby, the faster removal of As(III) could occur in early stage due to the above reason. On the other hand, under higher As initial concentration (>10 mg L^{-1}), with the increase of reaction time (after 12 h), the removal rate of As(V) increased progressively and finally exceeded that of As(III), which consisted with the q_{max} fitted from Langmuir model.

Furthermore, the As(III) and As(V) removal data were fitted by Temkin model, which as expressed in eqn (4), to prove the adsorption is spontaneous or not. In the equation, the T is the absolute temperature (K); $R = 8.314$ J mol K^{-1}, b_T is adsorption heat, and A_T is the maximum binding energy (L min^{-1}).

$$q_e = \frac{RT}{b_T} \ln(A_T C_e) \quad (4)$$

As seen from Fig. S3,† the removal data were fitted well by Temkin model, and the b_T got from curves is 295.12 J mol^{-1} and 201.23 J mol^{-1} for As(III) and As(V) removal, respectively. The b_T are both much greater than zero, indicating that the arsenic adsorption by CuFe$_2$O$_4$-foam/PMS couple is spontaneous.

Table 1 Langmuir and Freundlich isotherm parameters for As(III) and As(V) removal by the CuFe$_2$O$_4$-foam/PMS couple

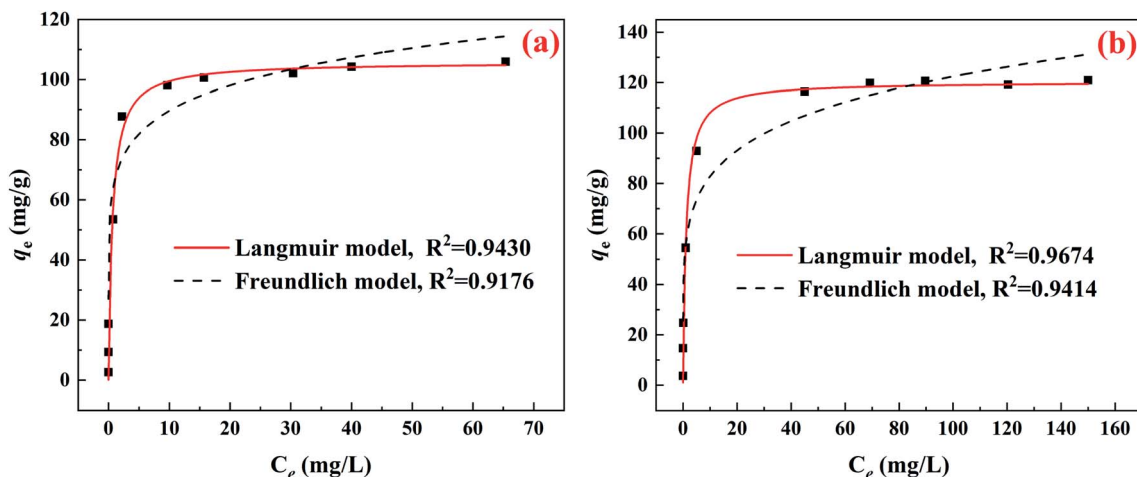|	Langmuir model			Freundlich model		
As	q_{max} (mg g^{-1})	K_L (L mg^{-1})	R^2	K_F (g mg^{-1})	n	R^2
As(III)	105.78	1.575	0.9430	66.43	7.69	0.9176
As(V)	120.32	0.875	0.9674	55.95	5.88	0.9414

Fig. 4 Removal isotherms for (a) As(III) and (b) As(V) by one piece of CuFe$_2$O$_4$-foam coupled with 100 μM PMS at pH$_0$ 7.0 under 25 °C.

3.3. Environmental implications

Both the reactivity and capacity of CuFe$_2$O$_4$-foam toward target contaminant determine the successful application of CuFe$_2$O$_4$-foam/PMS couple in wastewater treatment. To confirm the adsorptive property and stability of this system in practical application, after fulfilled adsorptive experiment, the CuFe$_2$O$_4$-foam was recovered and treated with 5% NaOH for 6 h (noted the mass loss is negligible). Furthermore, the removal capacity of As(III) was evaluated in consecutive runs. Considering the relatively low arsenic content in natural groundwater, the initial arsenic concentration of removal experiments was specified as 1 mg L^{-1}. Water samples were prepared through spiking with As(III) into pristine water sample (it was gathered from Hua Jing river in Wu Hu, China) to form a simulated waste water sample for removal experiments. It can be observed from Fig. 5a, the CuFe$_2$O$_4$-foam still maintained excellent adsorptive activity after seven successive cyclic runs of adsorption–desorption. The removal efficiency of As(III) is in the range of 100–99.4% within

10 min, and the residue As(III) concentration dropped dramatically from 1000 μg L^{-1} to 0–6 μg L^{-1}, which is lower than maximum contaminant level in drinking water (10 μg L^{-1}). A simple review on different spin Fe-based spinel particles as adsorbents for removing arsenic contaminant are presented in Table S1.† Comparatively, the higher arsenic adsorption capacity in this system than many other adsorbents.

On the other side, aiming to estimate the performance of CuFe$_2$O$_4$-foam for As(III) sequestration in continuous operation, up to 7 respikes of As(III) were performed on one batch of CuFe$_2$O$_4$-foam suspension. When As(III) was exhausted, 1 mL As(III) stock solution was added to the solution to achieve the similar As(III) concentration (∼1 mg L^{-1}). Likewise, as depicted in Fig. 5b, it was interesting that CuFe$_2$O$_4$-foam could adsorb As(III) rapidly in several consecutive runs. Although the rate constants for As(III) removal by CuFe$_2$O$_4$-foam/PMS couple decreased gradually from the first run to the seventh run, this couple held a higher reactivity toward As(III) even in the seventh
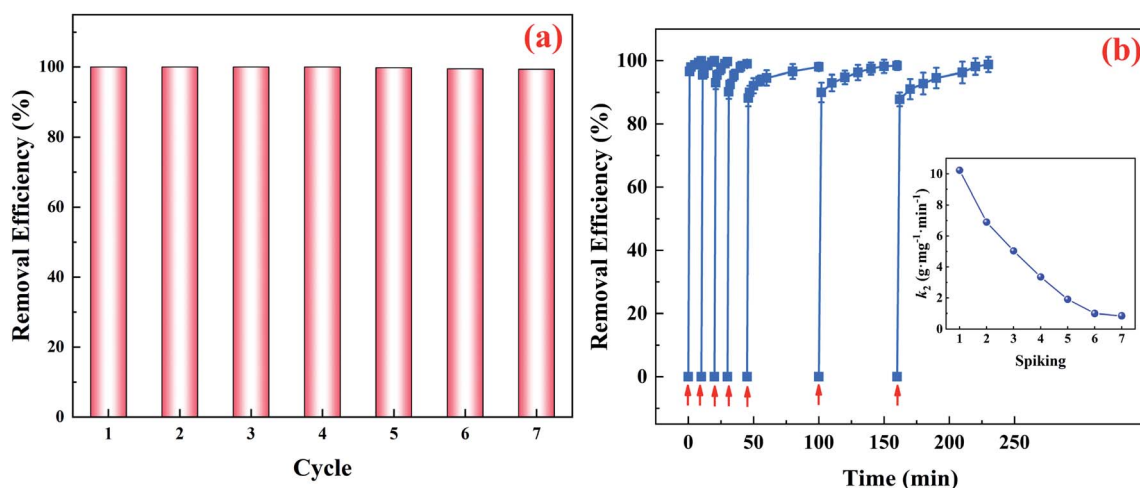

Fig. 5 Removal efficiency of As(III) in cyclic regeneration (a) and As(III) removal in consecutive runs (b) by CuFe$_2$O$_4$-foam/PMS couple. Inset: the rate constants. General conditions: one piece adsorbent, 100 μM PMS, pH 7.0, 25 °C, 1 mg L^{-1} As(III).

run than those of their counterparts $CuFe_2O_4$ without Fe–Ni framework supported in the first run (data not shown). Thereby, the application of $CuFe_2O_4$-foam will shorten time dramatically in the removal process in the real As(III)-contaminated groundwater treatment because it can maintain high removal capacity and efficiency even in seven consecutive uses without regeneration.

The potential change of adsorbent after seven cycles was measured by SEM, and XRD. Given that lower diffraction intensity is usually ascribed to crystallinity of the oxide,[39,40] the result clearly showed that no apparent changes of crystallinity of the used $CuFe_2O_4$ compared with the virgin one (Fig. S4†). The similar phenomenon was observed in SEM images of virgin and $CuFe_2O_4$ (Fig. S5†). The satisfactory removal efficiency can be obtained, although slight structural changes of materials in repeated cycles partly hinders the removal of arsenic, which can be avoided through properly prolonging the reaction time.

Due to rapid economic development and the growing industrial activities, there is an increases in the type and concentration of organic contaminants except for toxic inorganic pollutants (*e.g.* arsenic, chromium) in natural waters.[21] As seen from the above removal results, we can boldly predict that the $CuFe_2O_4$-foam/PMS couple has excellent oxidation potential. Hence, we have made a attempt that applied this couple to simultaneous remediation of organic pollutant (used methyl orange, MO) and adsorption of heavy metal, and the results presented in Fig. S6.† When MO and As(III) ions coexist, the $CuFe_2O_4$-foam/PMS couple exhibits a significant enhancement to the removal rate of MO and As(III), with nearly 100% removal within 50 min, compared to the pure $CuFe_2O_4$/PMS system. This work could be expected to the development of an attractive and reliable process for promoting the conversion and remediation of organic–inorganic contaminants. Stable Fe–Ni substrate and high catalytic activity of $CuFe_2O_4$ provide more possibility for the practical implications of this system in natural aquatic environments.

3.4. The effect of adsorbent and oxidant dosage

We secondly carried out systematic studies about the adsorbent and oxidant dosage to reveal the substantial impact of this couple on removal arsenic performance. The influence of $CuFe_2O_4$-foam and PMS dosage on arsenic removal were investigated at pH_0 7.0 and the results are depicted in Fig. 6. It is clearly shown that the increase in PMS dosage has a significant positive effect on As(III) removal, and the k_2 values increased from 0.0146 at 50 μM to 0.0286 g mg^{-1} min^{-1} at 400 μM. The enhancement for removal efficiency might result from faster oxidation of As(III) to As(v) when in presence of higher PMS concentration. Likewise, as shown in Fig. 6b, increasing $CuFe_2O_4$-foam dosage can remarkably enhance the kinetics of As(III) removal with k_2 values increased from 0.0085 (half piece) to 0.1632 g mg^{-1} min^{-1} (three pieces) in presence of 100 μM PMS, which could attributed to more adsorbent dosage would provide more adsorption sites. PMS-based AOPs are always considered complicated systems, and many factors influence their performance. Among of them, the self-consumption of PMS in the presence of high oxidation or catalyst dosage is great problem. Interestingly, there is no negative effect on arsenic removal within test scope of this experiment, no matter how much dosages of PMS and adsorbent were used for the reaction, which is different from the previous studies on heterogeneous catalysis for PMS.[25,41]

3.5. Effect of the solution chemistry

The influences of solution chemistry, such as initial pH, ubiquitous anions, natural organic matter and temperature on As(III) removal were evaluated at a fixed $CuFe_2O_4$-foam and PMS dosage since the rate of As(III) removal could be affected obviously by $CuFe_2O_4$-foam and PMS dosage based on the above results, and the data are presented in Fig. 7. The $CuFe_2O_4$-foam/PMS couple presents an appreciable As(III) removal efficiency under pH_0 3.0–9.0. Noted that natural groundwater generally has a neutral to slightly alkaline pH, which feature provides the
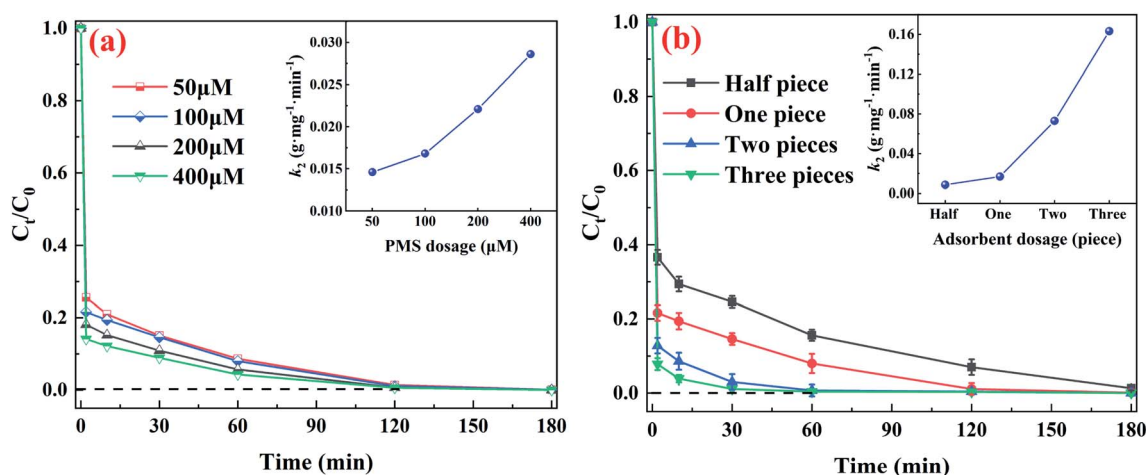

Fig. 6 The effect of different (a) PMS and (b) $CuFe_2O_4$-foam dosages for As(III) removal. General conditions: 10 mg L^{-1} As(III), pH 7.0, 25 °C, adsorbent: one piece for (a) and 100 μM PMS for (b).
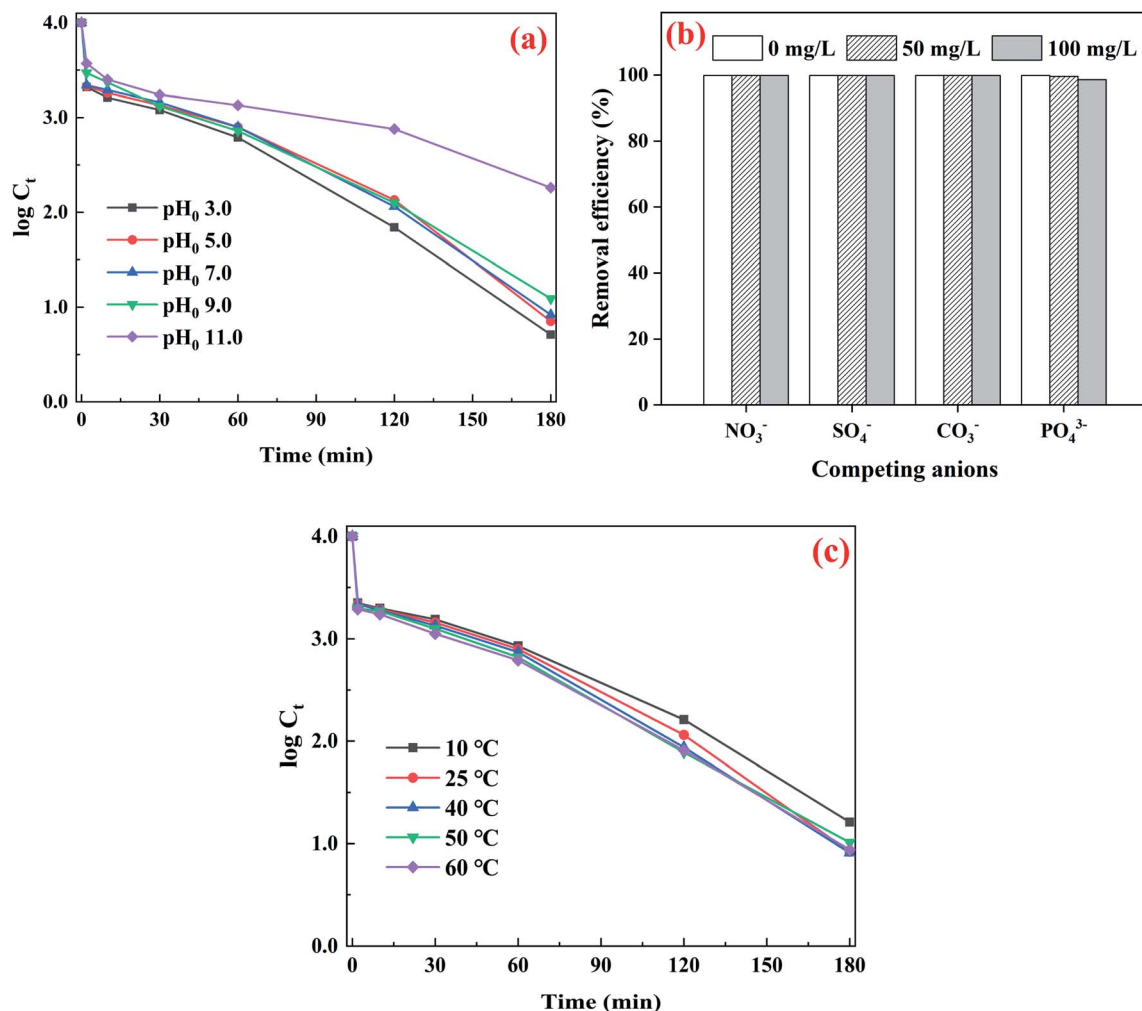
Fig. 7 Removal of As(III) by using CuFe$_2$O$_4$-foam/PMS couple as a function of (a) pH, (b) coexisting anions and (c) temperature. Inset: the rate constants. General conditions: 10 mg L^{-1} As(III), one piece adsorbent, 100 μM PMS, pH 7.0 for (b and c) and 25 °C for (a and b).

possibility for the practical application of the mixed system. While further increase of pH to 11, a slight decrease in rate constant of As(III) removal can be observed from the inset of Fig. 7a, which is possibly because the electrostatic repulsion between arsenate oxyanions (H$_2$AsO$_4^-$ and H$_2$AsO$_4^{2-}$) and adsorbents, of noted the pH$_{pzc}$ of the CuFe$_2$O$_4$-foam was around 7.7 (Fig. S7†). On the other hand, the main species is SO$_5^{2-}$ in PMS solution when pH was increased to strong alkaline (pK_{a1} < 0, pK_{a2} = 9.4), which might hinder its interaction with CuFe$_2$O$_4$-foam surface, thereby slightly reduced the generation of involved reactive species.

Fig. 7b presents the effect of some ubiquitous anions on the removal of arsenic. Generally, the presence of sulfate, nitrate and carbonate have negligible effect on As(III) removal even at anions concentration of 100 mg L^{-1}. It can be deduced from the formation of inner-sphere complex between As(III), the generated As(v) anions and the Fe-based adsorbents, whereas sulfate, nitrate and carbonate are mainly adsorbed by means of electrostatic attraction.[15,22] Comparatively, phosphate slightly suppressed As(III) uptake in the studied concentration ranges, that

is, the removal efficiency decreased from 99.9% (without phosphate) to 98.6% (with 100 mg L^{-1} phosphate) in the 180 min. The slight decrease of removal performance with the involvement of phosphate was probably attributed to the competition of binding sites between phosphate and arsenic, due to both of them can form inner-sphere complexes with the hydroxyl groups at the surface of adsorbents.[35,42] In contrast, such negative effect on As(III) removal was more significant than on As(v),[26] thus As(III) oxidation to As(v) by the PMS is obviously favorable for the subsequent removal of As(III) by CuFe$_2$O$_4$-foam. Compared to previous studies, the effect was less obviously,[22] because the load of CuFe$_2$O$_4$ on foam had changed As removal pathway compared with that of pristine CuFe$_2$O$_4$. Moreover, the HA, which representing the natural organic matter, presented negligible effect on As(III) removal even the addition of 50 mg L^{-1} (data not shown).

The effect of temperature on arsenic adsorption by CuFe$_2$O$_4$-foam/PMS couple is depicted in Fig. 7c. It is clearly shown that the increase with temperature has a slight positive effect on As(III) removal. The k_2 values from pseudo-second order model

increase from 0.0149 to 0.0203 g mg^{-1} min^{-1} with temperature increasing from 10 °C to 60 °C (Table S2†). The positive influence from temperature could be attributed to the improved mobility of As(III) from the liquid phase toward the solid surface at higher temperature, that is, the increased adsorption capacity or enhanced kinetic activity, specially the increase of reactive species for oxidation of As(III).[32,36,43]

3.6. Investigation of removal mechanism

To better elucidate the underlying sequestration mechanisms of As by prepared adsorbent, EDS elemental mapping of Fe, Ni, Cu, and As on As(III)-loading CuFe$_2$O$_4$-foam were obtained from FESEM images. As depicted in Fig. 8, the As elemental distribution is in line with Cu element, indicating that As was sequestrated by the embedded CuFe$_2$O$_4$ nanoparticles. This results revealed the possibility of synchronous oxidation and sequestration for As(III) by CuFe$_2$O$_4$-foam/PMS couple. Generally, the adsorption is effective only for As(v) but not valid for As(III).[10,44] Interestingly, as depicted in Fig. 9a, the CuFe$_2$O$_4$-foam/PMS couple presented higher adsorption efficiency for As(III). Nearly 100% As(III) removal was obtained within 180 min,

which much higher than that of As(v) (61.3%). More efficient As(III) removal could be ascribed to the synchronous oxidation and sequestration of As(III) by CuFe$_2$O$_4$-foam/PMS couple, which is more productive than the divided process of preoxidation and adsorption.[22] And the other reason may be the difference of K_L, which was discussed on the above section. We monitored the arsenic species in solution with the As(III) initial concentration of 10 mg L^{-1}, and the results are presented in Fig. 9b. The sharply decreased of As(III) concentration was observed within 2 min in solution, and the corresponding reaction rate was much higher than that of the As(v) generation, then the residual As(III) and As(v) was encapsulated progressively with the prolonged reaction time. Fast removal of As(III) and few generation of As(v) in solution further proved the underlying mechanism for As(III) by CuFe$_2$O$_4$-foam/PMS couple, that is, situ adsorption.

After As(III) uptake onto CuFe$_2$O$_4$-foam, its species on the solid sample were probed with the aid of XPS analysis. As depicted in Fig. S8,† the peak centered at 45.3 eV when in presence of PMS, revealing all the arsenic loaded in CuFe$_2$O$_4$-foam is in the form of As(v). In contrast, the more proportion of peak appearing at binding energy of 44.5 eV, which is arise from
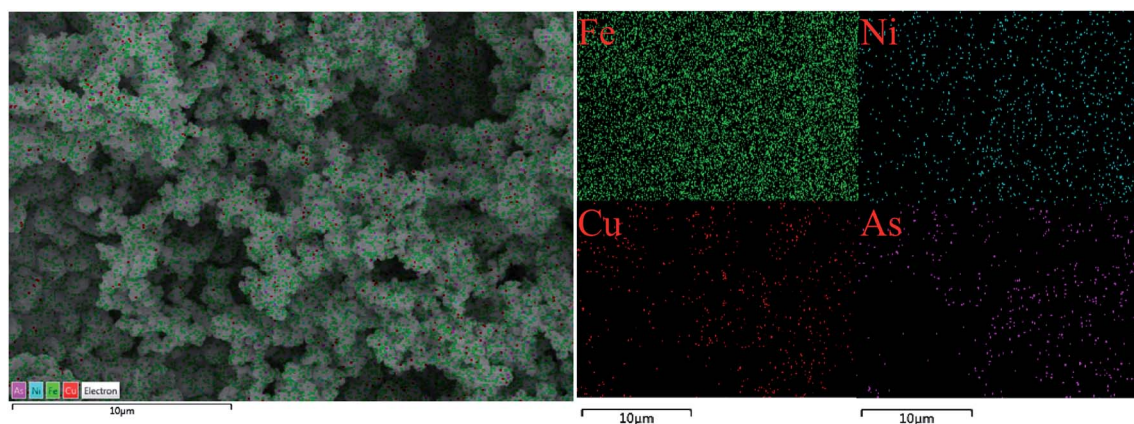

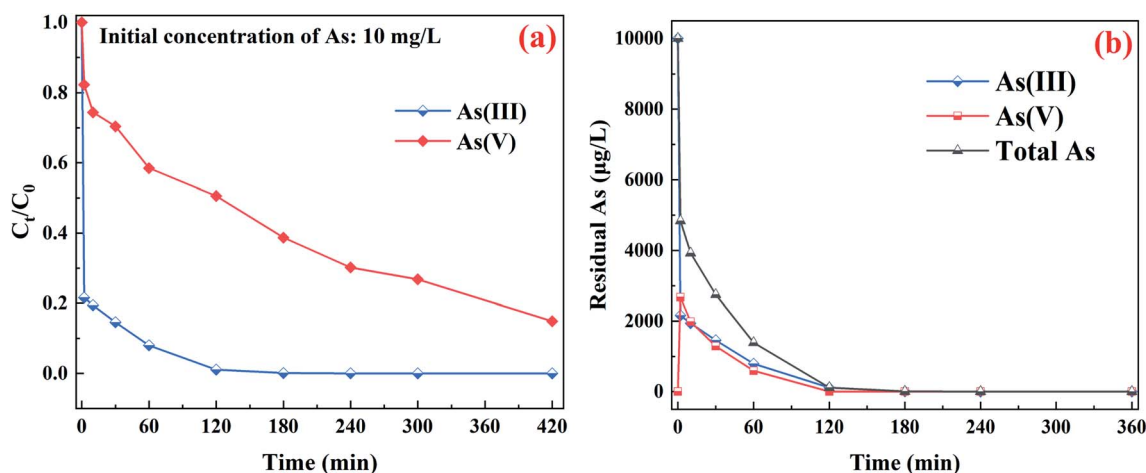**Fig. 8** SEM image of EDS spectra as elemental mapping of Fe, Ni, Cu, and As after As(III)-loading CuFe$_2$O$_4$-foam.

Fig. 9 (a) Removal kinetics of As(III) or As(v) by CuFe$_2$O$_4$-foam/PMS couple, and (b) arsenic species in solution with CuFe$_2$O$_4$-foam/PMS couple. Conditions: 10 mg L^{-1} As(III), 100 μM PMS, pH 7.0, 25 °C, one piece adsorbent.

As(III) species. Thus, the As(III) adsorption by $CuFe_2O_4$-foam/ PMS couple was finally completely transferred to As(v) in the solid phase by situ oxidation, whereas directly sequestered by the $CuFe_2O_4$-foam without PMS, the more proportion of species on adsorbent is As(III). Previous findings had revealed that sulfate radicals can be efficiently produced from PMS induced by many iron-based materials.[25,42,43] Therefore, to clarify the major radicals in this system, a series of radical scavenging experiments were carried out, and ethanol (EtOH) or *tert*-butyl alcohol (TBA) were used as quenchers.[44-47] The results are presented in Fig. S9,† as the EtOH, and TBA dosages increased, the removal rate of As(III) decreased progressively, which revealed the presence of ˙OH, $SO_4{}^{˙-}$. The results were consistent with the observations in previous study,[22,25] and thus the methods of anchoring has not change the production of radicals *via* $CuFe_2O_4$ catalyzing PMS.

The speciation of O element on the solid sample could further verify the above assumption. The surface hydroxyl groups (OH^-) on metal-based oxide are generally supposed to have a great influence on arsenic adsorption.[15,22] As presented in Fig. S10,† the ratio of OH^-/O of adsorbent increased from 43.8% (virgin) to 45.8% and 51.7% after $CuFe_2O_4$-foam alone and $CuFe_2O_4$-foam/PMS couple, respectively, which revealed the formation of monodentate mononuclear complexes. On the basis of the analysis of results above, the fast and efficient As(III) removal might be fulfilled through the following pathways: the first step is the sequestration of arsenic species by $CuFe_2O_4$-foam, accompanied by situ oxidation for As(III) in the presence of PMS. Afterwards, the inner-sphere species could produce between arsenic and adsorbent.

4. Conclusion

The strategy of anchoring $CuFe_2O_4$ on Fe–Ni framework to form porous $CuFe_2O_4$ foam can obviously reduce the agglomerated nature of nanoparticles. The prepared composite presents a dramatic removal capacity for arsenic, which is several times higher than that of bare $CuFe_2O_4$. These could be ascribed to the higher specific surface area, larger pore volume, more hydroxyl groups, and more accessible reactive sites of composite. Results showed that $CuFe_2O_4$-foam was effective for arsenic removal at a wide range of pH, and even in the presence of high concentration of ubiquitous anions. Synchronous oxidation and sequestration remarkably enhance the kinetics of As(III) sequestration when added PMS even as low as 50 μM. Moreover, the composite still retained excellent removal capacity after successively used for seven cycles whatever, which could be attributed to the stability of metal framework and high catalytic activity of $CuFe_2O_4$. The experimental results revealed that the loading of nanoparticles on metal foams is an effective way to improve their reactivity and adsorption ability, as such, it is believed to have great potential for environment applications.

Conflicts of interest

There are no conflicts to declare.

References

1 S. I. Siddiqui and S. A. Chaudhry, Iron oxide and its modified forms as an adsorbent for arsenic removal: a comprehensive recent advancement, *Process Saf. Environ. Prot.*, 2017, **111**, 592–626.

2 S. I. Siddiqui, M. Naushad and S. A. Chaudhry, Promising prospects of nanomaterials for arsenic water remediation: a comprehensive review, *Process Saf. Environ. Prot.*, 2019, **126**, 60–97.

3 O. X. Leupin, S. J. Hug and A. B. M. Badruzzaman, Arsenic removal from Bangladesh tube well water with filter columns containing zero valent iron filings and sand, *Environ. Sci. Technol.*, 2005, **39**, 8032–8037.

4 M. Argos, T. Kalra, P. J. Rathouz, Y. Chen, B. Pierce, F. Parvez, T. Islam, A. Ahmed, M. Rakibuz-Zaman, R. Hasan, G. Sarwar, V. Slavkovich, A. van Geen, J. Graziano and H. Ahsan, Arsenic exposure from drinking water, and all-cause and chronic-disease mortalities in Bangladesh (HEALS): a prospective cohort study, *Lancet*, 2010, **376**, 252–258.

5 L. Rodriguez-Lado, G. Sun, M. Berg, Q. Zhang, H. Xue, Q. Zheng and C. A. Johnson, Groundwater arsenic contamination throughout China, *Science*, 2013, **341**, 866–868.

6 J. G. Hering, I. A. Katsoyiannis, G. A. Theoduloz and M. Berg, Arsenic Removal from Drinking Water: Experiences with Technologies and Constraints in Practice, *J. Environ. Eng.*, 2017, **143**, 03117002.

7 R. Singh, S. Singh, P. Parihar, V. P. Singh and S. M. Prasad, Arsenic contamination, consequences and remediation techniques: A review, *Ecotoxicol. Environ. Saf.*, 2015, **112**, 247–270.

8 X. Hu, Z. Ding, A. R. Zimmerman, S. Wang and B. Gao, Batch and column sorption of arsenic onto iron-impregnated biochar synthesized through hydrolysis, *Water Res.*, 2015, **68**, 206–216.

9 J. H. Park, Y.-S. Han and J. S. Ahn, Comparison of arsenic co-precipitation and adsorption by iron minerals and the mechanism of arsenic natural attenuation in a mine stream, *Water Res.*, 2016, **106**, 295–303.

10 H.-J. Cui, J.-K. Cai, H. Zhao, B. Yuan, C.-L. Ai and M.-L. Fu, Fabrication of magnetic porous Fe–Mn binary oxide nanowires with superior capability for removal of As(III) from water, *J. Hazard. Mater.*, 2014, **279**, 26–31.

11 T. J. Sorg, A. S. C. Chen and L. Wang, Arsenic species in drinking water wells in the USA with high arsenic concentrations, *Water Res.*, 2014, **48**, 156–169.

12 C. K. Jain and I. Ali, Arsenic: occurrence, toxicity and speciation techniques, *Water Res.*, 2000, **34**, 4304–4312.

13 D. Wang, S. E. Gilliland III, X. Yi, K. Logan, D. R. Heitger, H. R. Lucas and W.-N. Wang, An Iron Mesh-Based Metal

Organic Framework Filter for Efficient Arsenic Removal, *Environ. Sci. Technol.*, 2018, **52**, 4275–4284.

14 G.-h. Moon, S. Kim, Y.-J. Cho, J. Lim, D.-h. Kim and W. Choi, Synergistic combination of bandgap-modified carbon nitride and WO$_3$ for visible light-induced oxidation of arsenite accelerated by in situ Fenton reaction, *Appl. Catal., B*, 2017, **218**, 819–824.

15 X. Zhang, M. Wu, H. Dong, H. Li and B. C. Pan, Simultaneous Oxidation and Sequestration of As(III) from Water by Using Redox Polymer-Based Fe(III) Oxide Nanocomposite, *Environ. Sci. Technol.*, 2017, **51**, 6326.

16 Y. Bai, T. Yang, J. Liang and J. Qu, The role of biogenic Fe-Mn oxides formed *in situ* for arsenic oxidation and adsorption in aquatic ecosystems, *Water Res.*, 2016, **98**, 119–127.

17 C. Zhang, Y. Xiao, Y. Qin, Q. Sun and S. Zhang, A novel highly efficient adsorbent {[Co$_4$(L)$_2$(μ_3-OH)$_2$(H$_2$O)$_3$(4,4′-bipy)$_2$]·(H$_2$O)$_2$}$_n$: synthesis, crystal structure, magnetic and arsenic(V) absorption capacity, *J. Solid State Chem.*, 2018, **261**, 22–30.

18 L.-K. Wu, H. Wu, H.-B. Zhang, H.-Z. Cao, G.-Y. Hou, Y.-P. Tang and G.-Q. Zheng, Graphene oxide/CuFe$_2$O$_4$ foam as an efficient absorbent for arsenic removal from water, *Chem. Eng. J.*, 2018, **334**, 1808–1819.

19 L. Önnby, P. S. Kumar, K. G. V. Sigfridsson, O. F. Wendt, S. Carlson and H. Kirsebom, Improved arsenic(III) adsorption by Al$_2$O$_3$ nanoparticles and H$_2$O$_2$: evidence of oxidation to arsenic(V) from X-ray absorption spectroscopy, *Chemosphere*, 2014, **113**, 151–157.

20 D. H. Kim, A. D. Bokare, S. K. Min and W. Choi, Heterogeneous Catalytic Oxidation of As(III) on Nonferrous Metal Oxides in the Presence of H$_2$O$_2$, *Environ. Sci. Technol.*, 2015, **49**, 3506.

21 Y.-G. Kang, H. Yoon, W. Lee, E.-j. Kim and Y.-S. Chang, Comparative study of peroxide oxidants activated by nZVI: Removal of 1,4-Dioxane and arsenic(III) in contaminated waters, *Chem. Eng. J.*, 2018, **334**, 2511–2519.

22 Y. Wei, H. Liu, C. Liu, S. Luo, Y. Liu, X. Yu, J. Ma, K. Yin and H. Feng, Fast and efficient removal of As(III) from water by CuFe$_2$O$_4$ with peroxymonosulfate: Effects of oxidation and adsorption, *Water Res.*, 2019, **150**, 182–190.

23 Z. Li, C. Guo, J. Lyu, Z. Hu and M. Ge, Tetracycline degradation by persulfate activated with magnetic Cu/CuFe$_2$O$_4$ composite: Efficiency, stability, mechanism and degradation pathway, *J. Hazard. Mater.*, 2019, **373**, 85–96.

24 N. Masunga, O. K. Mmelesi, K. K. Kefeni and B. B. Mamba, Recent advances in copper ferrite nanoparticles and nanocomposites synthesis, magnetic properties and application in water treatment: Review, *J. Environ. Chem. Eng.*, 2019, **7**, 103179.

25 X. Dong, B. Ren, Z. Sun, C. Li, X. Zhang, M. Kong, S. Zheng and D. D. Dionysiou, Monodispersed CuFe$_2$O$_4$ nanoparticles anchored on natural kaolinite as highly efficient peroxymonosulfate catalyst for bisphenol A degradation, *Appl. Catal., B*, 2019, **253**, 206–217.

26 L.-K. Wu, H. Wu, H.-B. Zhang, H.-Z. Cao, G.-Y. Hou, Y.-P. Tang and G.-Q. Zheng, Graphene oxide/CuFe$_2$O$_4$ foam

as an efficient absorbent for arsenic removal from water, *Chem. Eng. J.*, 2018, **334**, 1808–1819.

27 Y. Wang, H. Zhao, M. Li, J. Fan and G. Zhao, Magnetic ordered mesoporous copper ferrite as a heterogeneous Fenton catalyst for the degradation of imidacloprid, *Appl. Catal., B*, 2014, **147**, 534–545.

28 Y. Yao, Y. Cai, F. Lu, F. Wei, X. Wang and S. Wang, Magnetic recoverable MnFe$_2$O$_4$ and MnFe$_2$O$_4$–graphene hybrid as heterogeneous catalysts of peroxymonosulfate activation for efficient degradation of aqueous organic pollutants, *J. Hazard. Mater.*, 2014, **270**, 61–70.

29 T. Xu, G. He, Y. Zhao, H. Gu, Z. Jiang, Q. Chen, X. Sun and H. Chen, Benzenoid-like CuFeO$_2$@reduced graphene oxide: Facile synthesis and its excellent catalytic performance in selective oxidation, *Appl. Surf. Sci.*, 2016, **389**, 840–848.

30 X. Zhang, M. Feng, R. Qu, H. Liu, L. Wang and Z. Wang, Catalytic degradation of diethyl phthalate in aqueous solution by persulfate activated with nano-scaled magnetic CuFe$_2$O$_4$/MWCNTs, *Chem. Eng. J.*, 2016, **301**, 1–11.

31 Z. Chen, L. Wang, H. Xu and Q. Wen, Efficient heterogeneous activation of peroxymonosulfate by modified CuFe$_2$O$_4$ for degradation of tetrabromobisphenol A, *Chem. Eng. J.*, 2020, **389**, 124345.

32 L. K. Wu, H. Wu, Z. Z. Liu, H. Z. Cao, G. Y. Hou, Y. P. Tang and G. Q. Zheng, Highly porous copper ferrite foam: A promising adsorbent for efficient removal of As(III) and As(V) from water, *J. Hazard. Mater.*, 2018, **347**, 15–24.

33 Z. Wang, R. T. Bush, L. A. Sullivan, C. Chen and J. Liu, Selective Oxidation of Arsenite by Peroxymonosulfate with High Utilization Efficiency of Oxidant, *Environ. Sci. Technol.*, 2014, **48**, 3978–3985.

34 S. Luo, S. Yang, X. Wang and C. Sun, Reductive degradation of tetrabromobisphenol A over iron–silver bimetallic nanoparticles under ultrasound radiation, *Chemosphere*, 2010, **79**, 672–678.

35 D. Wu, S. Peng, K. Yan, B. Shao, Y. Feng and Y. Zhang, Enhanced As(III) Sequestration Using Sulfide-Modified Nano-Scale Zero-Valent Iron with a Characteristic Core–Shell Structure: Sulfidation and As Distribution, *ACS Sustainable Chem. Eng.*, 2018, **6**, 3039–3048.

36 S. Luo, S. Yang, X. Wang and C. Sun, Reductive degradation of tetrabromobisphenol A over iron–silver bimetallic nanoparticles under ultrasound radiation, *Chemosphere*, 2010, **79**, 672–678.

37 Z. Zhou, Y. Zhang, Z. Wang, W. Wei, W. Tang, J. Shi and R. Xiong, Electronic structure studies of the spinel CoFe$_2$O$_4$ by X-ray photoelectron spectroscopy, *Appl. Surf. Sci.*, 2008, **254**, 6972–6975.

38 Q. Lan, A. S. Bassi, J.-X. Zhu and A. Margaritis, A modified Langmuir model for the prediction of the effects of ionic strength on the equilibrium characteristics of protein adsorption onto ion exchange/affinity adsorbents, *Chem. Eng. J.*, 2001, **81**, 179–186.

39 S. Azabou, W. Najjar, A. Gargoubi, A. Ghorbel and S. Sayadi, Catalytic wet peroxide photo-oxidation of phenolic olive oil mill wastewater contaminants: Part II. Degradation and

detoxification of low-molecular mass phenolic compounds in model and real effluent, *Appl. Catal., B*, 2007, **77**, 166–174.

40 D. Ding, C. Liu, Y. Ji, Q. Yang, L. Chen, C. Jiang and T. Cai, Mechanism insight of degradation of norfloxacin by magnetite nanoparticles activated persulfate: Identification of radicals and degradation pathway, *Chem. Eng. J.*, 2017, **308**, 330–339.

41 D. Miao, J. Peng, M. Wang, S. Shao, L. Wang and S. Gao, Removal of atorvastatin in water mediated by $CuFe_2O_4$ activated peroxymonosulfate, *Chem. Eng. J.*, 2018, **346**, 1–10.

42 Y. Xu, Z. Lin, Y. Zheng, J. P. Dacquin, S. Royer and H. Zhang, Mechanism and kinetics of catalytic ozonation for elimination of organic compounds with spinel-type $CuAl_2O_4$ and its precursor, *Sci. Total Environ.*, 2019, **651**, 2585–2596.

43 C. Tan, N. Gao, Y. Deng, W. Rong, S. Zhou and N. Lu, Degradation of antipyrine by heat activated persulfate, *Sep. Purif. Technol.*, 2013, **109**, 122–128.

44 F. liu, W. M. Yang, W. W. Li and G.-C. Zhao, Simultaneous Oxidation and Sequestration of Arsenic(III) from Aqueous Solution by Copper Aluminate with Peroxymonosulfate: A Fast and Efficient Heterogeneous Process, *ACS Omega*, 2021, DOI: 10.1021/acsomega.0c05203.

45 G. P. Anipsitakis and D. D. Dionysiou, Degradation of organic contaminants in water with sulfate radicals generated by the conjunction of peroxymonosulfate with cobalt, *Environ. Sci. Technol.*, 2003, **37**, 4790–4797.

46 C. Liang and H.-W. Su, Identification of Sulfate and Hydroxyl Radicals in Thermally Activated Persulfate, *Ind. Eng. Chem. Res.*, 2009, **48**, 5558–5562.

47 G. P. Anipsitakis and D. D. Dionysiou, Radical generation by the interaction of transition metals with common oxidants, *Environ. Sci. Technol.*, 2004, **38**, 3705–3712.